energies

MDPI

Article

Electromagnetic Interference in a Buried Multiconductor Cable Due to a Dynamic Wireless Power Transfer System

Silvano Cruciani [1], Tommaso Campi [2,*], Francesca Maradei [1] and Mauro Feliziani [2]

[1] Department of Astronautics, Electrical and Energetics Engineering, Sapienza University of Rome, 00185 Rome, Italy; silvano.cruciani@uniroma1.it (S.C.); francesca.maradei@uniroma1.it (F.M.)
[2] Department of Industrial and Information Engineering and Economics, University of L'Aquila, 67040 L'Aquila, Italy; mauro.feliziani@univaq.it
* Correspondence: tommaso.campi@univaq.it

Abstract: The aim of this study is to predict the electromagnetic interference (EMI) effect produced by a dynamic wireless power transfer (DWPT) system on a buried multiconductor signal cable. The short-track DWPT system architecture is here considered with an operating frequency of 85 kHz and maximum power transferred to an EV equal to 10 kW. The EMI source is the DWPT transmitting coil which is activated when a vehicle passes over it. The electric and magnetic fields in the earth produced by the DWPT coil currents are calculated numerically using the finite elements method (FEM). These fields are then used to derive the voltage and current sources that appear in the field-excited multiconductor transmission line (MTL) model, used for the buried shielded cable. The MTL is analyzed considering the first ten harmonics of the current. The currents and voltages at the terminal ends are calculated considering the wireless charging of a single electric vehicle (EV) first, and then the simultaneous charging of 10 EVs which absorb a total power of 100 kW. The preliminary results reveal possible EMI problems in underground cables.

Keywords: wireless power transfer (WPT); dynamic wireless power transfer (DWPT); electromagnetic interference (EMI); conducted emission (CE); multiconductor transmission line (MTL); e-mobility

Citation: Cruciani, S.; Campi, T.; Maradei, F.; Feliziani, M. Electromagnetic Interference in a Buried Multiconductor Cable Due to a Dynamic Wireless Power Transfer System. *Energies* **2022**, *15*, 1645. https://doi.org/10.3390/en15051645

Academic Editor: Haifeng Dai

Received: 21 January 2022
Accepted: 21 February 2022
Published: 23 February 2022

1. Introduction

The development of dynamic wireless charging for electric vehicles (EVs) is a key aspect for the future of autonomous transportation systems. Nowadays, the EVs are recharged when the vehicle is stationary, e.g., parked in a garage at home or in a charging station located along the road, and the electricity is transferred from the electric grid to EVs mainly using a plug-in connection. Currently, the main limitation of EVs is the limited energy that can be stored in the battery. This results in a limited range for EVs compared to traditional petrol-fueled vehicles. Another disadvantage is the long time required to significantly recharge the battery when connected to a charging station (either wired or wireless). A stationary wireless power transfer (WPT) system is a viable alternative to the current plug-in solution, offers the advantage of increased safety and allows you to fully automate the charging process without the need for any human interaction. However, even the stationary WPT does not solve the problems of autonomy and charging time.

Automotive dynamic wireless transfer power (DWPT) is a recent development of the WPT technology that allows to transfer electric power to an EV when it is moving along an electrified road [1–4]. This technology allows the EV to ideally achieve an 'infinite' autonomy as long as the roads are equipped with DWPT charging tracks. While this technology is extremely promising, it presents several issues including electromagnetic compatibility (EMC) problems with other electrical infrastructures. The aim of this work is to investigate the electromagnetic interference (EMI) produced by a DWPT system with a short track configuration on an underground multiconductor signal cable. In this type of

DWPT architecture, the transmitting coils are not activated continuously and, as a result, transients occur that can generate EMI. In addition, power electronic converters, such as inverters and rectifiers usually present in the DWPT system, are possible sources of interference. For both reasons the induced effects on the buried cable are not limited at the frequency used for WPT, but also higher order harmonics of current are produced.

In this study, we present a method based on the multiconductor transmission line (MTL) theory to evaluate the induced currents and voltages produced by a DWPT system in an underground signal cable such as those used for traffic lights. It is composed of an external conductive armor and several inner conductors. It should be noted that the topic of the paper is very new, as DWPT systems have not yet been implemented in the real world, but only demonstrated in experimental projects. There are several technological problems in the development of DWPT systems, but one of the critical problems is the possible EMI in other electrical systems located in the vicinity of the electrified road. Therefore, simulation studies such as the one here presented are very important to preliminarily investigate the possible side effects of this technology for which real EMC/EMI tests are not yet possible.

The paper is organized as described below. Section 2 describes first the configuration of the DWPT system used for the simulations, and then presents the MTL equations for the analysis of the effects induced in a multi-conductor buried cable. Great attention is also paid to the magnetic coupling model between DWPT coils and underground cables.

In Section 3 the models previously proposed are applied, obtaining some significant results in terms of currents and voltages induced at the terminal ends of the buried cable. The results obtained are validated by comparison with other methods. The EMI in the cable is examined in the case of a single vehicle being wireless charged, but also for 10 vehicles simultaneously present that absorb a total power of 100 kW.

2. Materials and Methods

2.1. System Configuration

A DWPT system is considered assuming the operational frequency equal to 85 kHz and the maximum power transferred to an EV equal to 10 kW. The dynamic WPT system here considered is composed by a series of short track transmitting coils embedded in the road while the receiving coil is mounted on the underneath of the EV. Each transmitting coil is activated only for the period in which the vehicle is over the coil itself. An electronic unit controls the activation process of transmitting coils to maximize the coupling. The coil configuration considered here is taken from the European Project FABRIC [1]. The ground assembly (GA) is a planar coil with rectangular shape of dimensions 150 cm × 50 cm with 10 turns. The vehicle assembly (VA) is a planar coil of dimensions 40 cm × 62 cm composed by 10 turns. Two ferrite blocks of dimensions 15 cm × 25 cm × 0.5 cm are placed in proximity of the VA coil. The average vertical distance between the GA and the VA coils is assumed equal to h = 20 cm. The coils are realized using a Litz wire composed of 1260 strands of insulated wires of dimension AWG 38. A sketch of the system is shown in Figure 1.

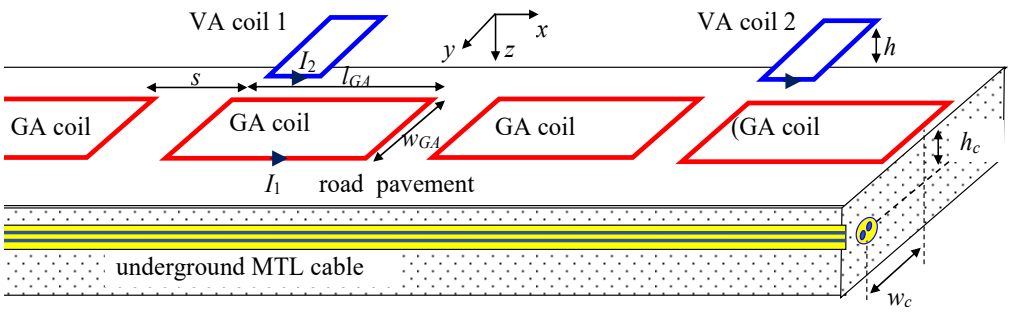

Figure 1. System configuration.

The implementation site of the DWPT system considered is an urban environment with a maximum speed limit of 50 km/h. This means that the travel time of a vehicle over a GA coil of length l_{GA} = 1.5 m is approximately equal to 0.1 s, while the period of a sinusoidal signal operating at 85 kHz is 11.7 µs. Consequently, the time constant due to the movement of the vehicle is about 4 orders of magnitude higher than the electrical time constant. It means that the cruising speed of the EV does not greatly affect the EMI which is mainly due to the DWPT operations. Transients are also produced by the activation/deactivation of the transmitting coils due to the movement of the vehicle.

2.2. Multiconductor Trasmission Line Theory Applied to Induced Currents in Buried Wires

The aim of the proposed study is to quantify the EMI in an underground signal cable when it is exposed to the electromagnetic field produced by the DWPT coils. The cable is modeled as a uniform multiconductor transmission line (MTL) excited by the non-uniform field generated by the DWPT coils. A typical configuration is schematically shown in Figure 1. The voltage and current wave propagation is modeled using the field-excited MTL equations [5]:

$$-\frac{d[V]}{dx} = [Z][I] - [E] \tag{1}$$

$$-\frac{d[I]}{dx} = [Y][V] - [J] \tag{2}$$

where $[Z]$ and $[Y]$ are the p.u.l. impedance and admittance matrices, $[V]$ and $[I]$ are the voltage and current vectors, $[E]$ and $[J]$ are the p.u.l. voltage and current source vectors [5]. Matrices $[Z]$ and $[Y]$ can be either calculated using numerical simulations [6] or can be analytically derived for simple configurations [7].

The parameters $[Z]$ and $[Y]$ are calculated with the two-dimensional (2D) FEM using the magnetoquasistatic (MQS) and the electrostatic (ES) solvers. The MQS formulation in 2D is based on the solution of the following Equations [8,9]:

$$\nabla \times \frac{1}{\mu}\nabla \times \mathbf{A} + j\omega\sigma\mathbf{A} = \mathbf{J_e} \tag{3a}$$

$$\mathbf{B} = \nabla \times \mathbf{A} \tag{3b}$$

$$\mathbf{E} = -j\omega\mathbf{A} \tag{3c}$$

where $\omega = 2\pi f$, μ is the magnetic permeability (unit of measure: H/m), σ is the electrical conductivity (S/m), $\mathbf{J_e}$ is the current source density (A/m), $\mathbf{E}$ is the electric field (V/m) and $\mathbf{A}$ is the magnetic vector potential (Wb/m). The electrostatic (ES) formulation is based on the solution of the following 2D Equations [8,9]:

$$\nabla \cdot \varepsilon\mathbf{E} = \rho \tag{4a}$$

$$E = -\nabla V \tag{4b}$$

where ε is the dielectric permittivity (F/m), ρ the space charge density (C/m^3) and V the electric potential (V). Using the FEM MQS approximation the matrix, $[Z]$ can be calculated with a number of steps equal to the number N of the conductors [6]. Since the coefficients of $[Z]$ are frequency-dependent due to skin and proximity effects, the procedure is repeated for each one of the frequencies of interest. The matrix $[Y]$ is calculated using an ES solver. The procedure is composed by N steps: on each step a potential equal to 1 V is imposed on the surface of each conductors and 0 V on the others ($V_i = 1,\ V_j = 0$ for $j = 1, \ldots, N$ and $j \neq i$).

Considering that the signal cable is buried, the voltages are referred to the zero voltage plane taken at an infinite distance underground. This plane is also considered as the return path of the currents.

If the cable is shielded, the equivalent circuit is composed by an external mesh and n internal meshes, being n the number of the inner wires, as shown in Figure 2 for an MTL shielded cable with $n = 2$. The total number of independent conductors is $N = n + 1$ and the order of matricial telegraphers' equations is N. The external mesh is composed by the external shield and the current return path, while the internal meshes are composed by the n inner wires and the internal shield. The external mesh and the internal meshes are coupled by the shield transfer impedance and admittance.

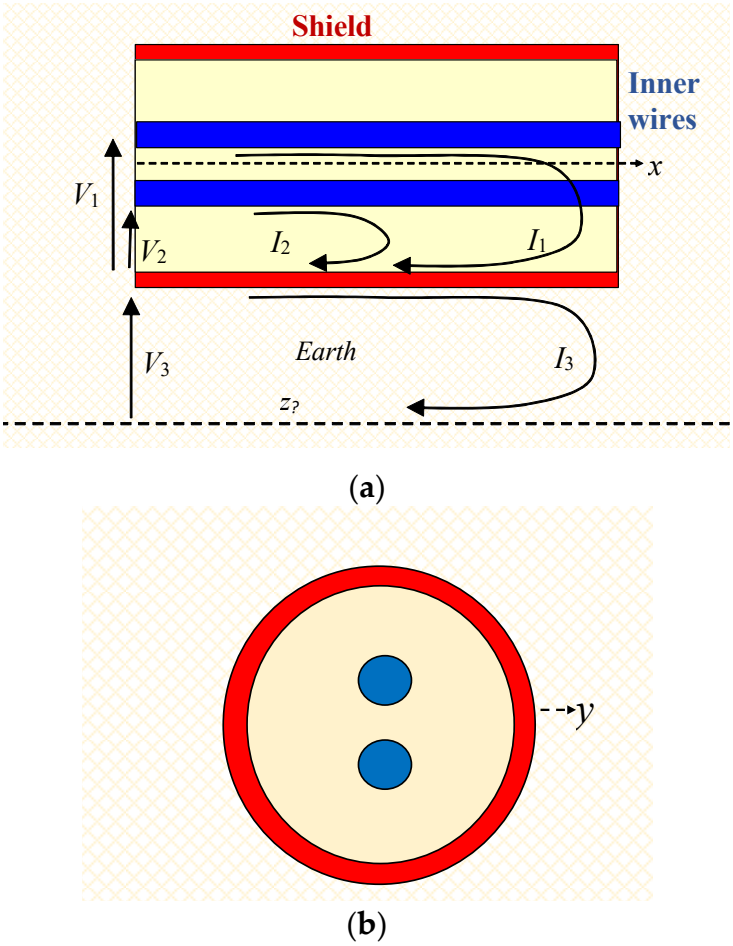

Figure 2. Sketch of the currents in an MTL shielded cable (**a**) and cable cross-section (**b**).

The MTL equations of a field-excited multiconductor shielded cable can be rewritten as [10–13]:

$$-\frac{d}{dx}\begin{bmatrix}[V_w(x)]\\ V_s(x)\end{bmatrix} = \begin{bmatrix}[Z_w] & [1]Z_t\\ [0]^T & Z_s\end{bmatrix}\begin{bmatrix}[I_w(x)]\\ I_s(x)\end{bmatrix} - \begin{bmatrix}[0]\\ E_{ext}(x)\end{bmatrix} \tag{5a}$$

$$-\frac{d}{dx}\begin{bmatrix}[I_w(x)]\\ I_s(x)\end{bmatrix} = \begin{bmatrix}[Y_w] & [1]Y_t\\ [0]^T & Y_s\end{bmatrix}\begin{bmatrix}[V_w(x)]\\ V_s(x)\end{bmatrix} - \begin{bmatrix}[0]\\ J_{ext}(x)\end{bmatrix} \tag{5b}$$

where x is the line axis, $[V_w]$ is the vector of the n voltages between inner wires and the internal shield, $[I_w]$ is the vector of the currents flowing into the n inner wires, V_s is the external shield voltage, I_s is the current flowing into the external shield, $[Z_w]$ and $[Y_w]$ are the p.u.l. impedance and admittance matrices of the internal meshes (i.e., inner wires–internal shield), Z_s and Y_s are the p.u.l. impedance and admittance of the external mesh (i.e., external shield–reference plane), Z_t and Y_t are the p.u.l. transfer impedance and admittance of the shield, [0] and [1] are column vector of size $n \times 1$ composed by 0 and 1, respectively.

The MTL excitation is given by the distributed voltage and current sources E_{ext} and J_{ext} [13]:

$$E_{ext} = -j\omega \int_{z_{-\infty}}^{z_j} B_y dz \tag{6a}$$

$$J_{ext} = -Y_j \int_{z_{-\infty}}^{z_j} E_z dz \tag{6b}$$

B_y being the transversal component of the magnetic flux density and E_z is the vertical electric field, both produced by the DWPT coils, and Y_j is the admittance of the circuit mesh given by the external shield and the reference plane. The integrals in (6a) and (6b) are calculated on a line from z_j (z-coordinate of the jth conductor) to $-\infty$ (here assumed $z_{-\infty} = -30$ m for the numerical calculation). For the calculation of the excitations in (6) a FEM MQS simulation is performed for each of the frequencies of interest.

It should be noted that the impedances Z_s and the admittance Y_s are given by [14,15]:

$$Z_s = Z_g + Z_{se} \tag{7}$$

$$Y_s = Y_g \tag{8}$$

Z_g being the ground impedance, Y_g the ground admittance and Z_{se} the external shield impedance. The expressions of all impedance and admittance in (5)–(8) can be found in the technical literature [14–19]. The solution of MTL equations in the frequency domain is well established and it is not original. The novelty of the paper is in the excitation system of the underground cable which is given by the electromagnetic field produced by the coils of the DWPT system. Since the coils are not uniformly distributed and the DWPT architecture is based on short tracks, it follows that the excitation is intermittent and occurs at different points along the multiconductor cable due to the movement of the electric vehicles along the electrified road. This leads to a nonuniform excitation of the MTL cable. The nonuniform excitation is modeled as a series cascade of different MTL sections, excited and non-excited. The excited sections of the MTL cable correspond to the GA coil activated due to the presence of a charging EV, while the non-excited sections are all other sections without EVs. To simplify the study, the length of the excited cable section corresponds to that of the activated GA coil, l_{GA}. A scheme of the cable excitation is shown in Figure 3. The equivalent circuit consisting of several sections of cable in series cascaded can be analyzed by solving the MTL equations after applying the terminal conditions. The equivalent circuit can also be analyzed by a CAD circuit simulator such as SPICE.

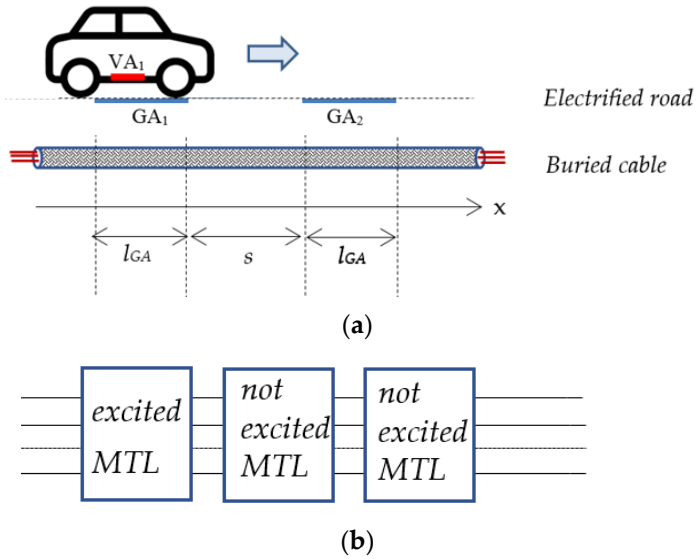

Figure 3. Scheme of excited and non-excited MTL sections. (**a**) Geometrical configuration. (**b**) Series cascade of MTL sections.

3. Results

3.1. Cable Configuration

The cable under study is a traffic light cable, buried inside the road pavement at a depth of h_c = 50 cm, and parallel to the electrified road at a lateral distance w_c = 75 cm with respect to the center of the GA coils. The traffic light cable is made up of n = 8 internal copper conductors with a section of 1 mm^2, as shown in Figure 4. The thickness of the insulation of each conductor is t_1 = 0.6 mm, the thickness of the internal and external insulations are t_2 = 0.8 and t_3 = 1.4 mm, respectively. The aluminum shield (armor) placed between the external and internal insulation has a thickness of t_s = 0.9 mm. For simplicity and for the frequencies of interest, the shield is assumed to be solid. The total external diameter of the cable is d_w = 14 mm. In the calculation of the magnetic and electric fields produced by the DWPT coils, the earth surrounding the cable is modeled assuming μ_r = 1, ε_r = 10 and σ = 10 mS/m.

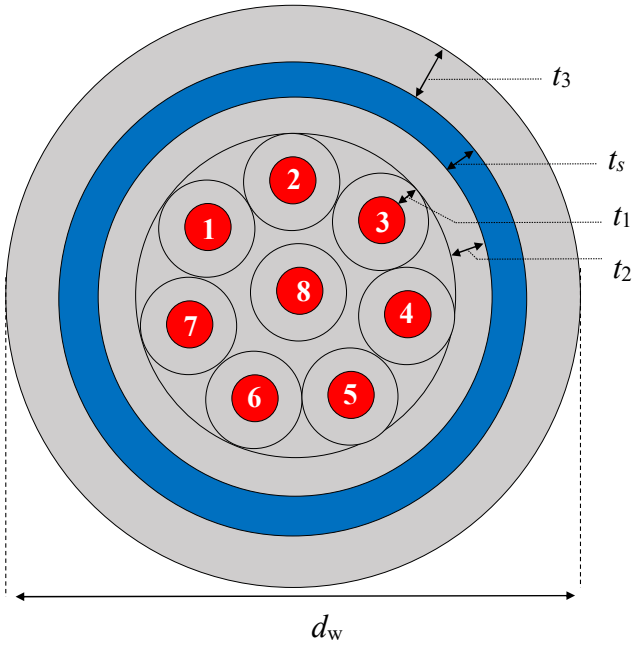

Figure 4. Cross-section of MTL cable with numbered conductors.

3.2. MTL Excitation

The MTL excitation, given by (5) and (6), depends on the electric and magnetic field produced by the currents flowing in the DWPT coils. Therefore, first of all it is necessary to know the coil currents flowing in an equivalent circuit of the WPT system. On the transmitting side, the WPT circuit is composed of an inverter that provides the high frequency signal operating at 85 kHz. On the receiving side the WPT circuit is composed of a full-bridge AC-DC converter and a capacitor for further smoothing of the current, and of a battery [20–22]. The transmitting and receiving sides are coupled by two inductors which are also compensated by capacitors. The equivalent circuit of the WPT system described above is shown in Figure 5 (the primary side of the DWPT system is shown in Figure 5a, the receiving circuit is shown in Figure 5b, the two inductors L_p and L_s are coupled by the coupling coefficient k which is not shown in the figure). The self-inductances of the coils are L_p = 348 µH and L_s = 195 µH, and their coupling coefficient is k = 0.07. The coils' resistances are obtained from the datasheet of the considered Litz wire and are R_p = 350 mΩ and R_s = 175 mΩ. The series capacitances C_p =10 nF and C_s =18 nF are chosen to make the system resonant at the operating frequency of 85 kHz. The inverter has a full bridge configuration with a MOSFETs switch. Each MOSFET is driven by a square voltage source that permits to introduce a dead-time between the commutation of the high side and low-side switches, to avoid a short circuit. On the receiving side, the AC-DC conversion is

performed with four Schottky diodes in full configuration. Finally, a capacitor C_f is used to smooth the output voltage.

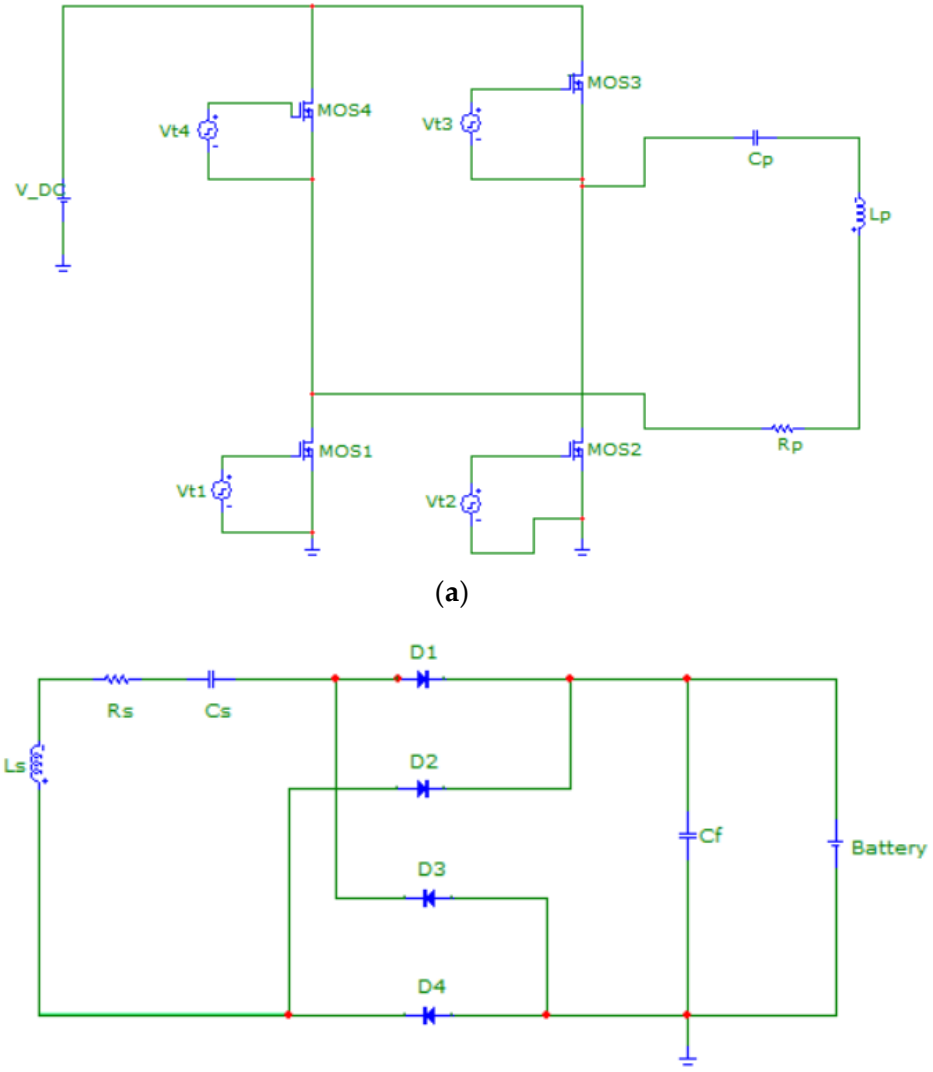

Figure 5. SPICE model of GA coil (**a**) and VA coil (**b**) (the coupling of inductors L_p and L_s by k is not shown in the figure).

The equivalent circuit is analyzed by a SPICE circuit simulator and the time-domain currents flowing in the inductances L_p and L_s are transformed in the frequency domain using the Fast Fourier Transform (FFT). The first harmonic corresponds to 85 kHz and the first ten current harmonics are considered for the calculation of the induced effects on the buried cable [4].

The SPICE solution in time domain of the current in the GA coil is reported in Figure 6a while the absolute value of the first ten odd harmonics of the GA coil current are shown in Figure 6b. These current values are the sources of the electric and magnetic fields in (6). The fields are calculated in the frequency-domain by a 3D FEM simulation of the DWPT installation, considering also the presence of a vehicle just above the GA coil. The vehicle bottom is modeled by an aluminum plate with dimensions 3.5 m $\times$ 1.7 m and thickness equal to 5 mm [4]. The presence of the aluminum plate modifies the resistances and inductances of the DWPT circuit and the distribution of the electric and magnetic fields. The WPT configuration is analyzed using a 3D FEM simulation [23–25] at the frequencies

corresponding to the first ten odd harmonics of current. In the calculations the fields produced by the VA coil are assumed to be negligible since their contributions in (6) are significantly smaller than those produced by the GA coil due to a smaller current and a higher distance.

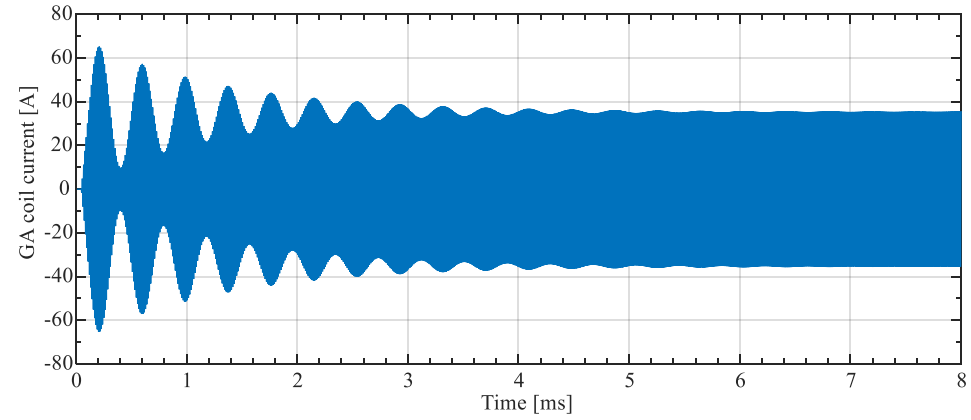

(**a**)

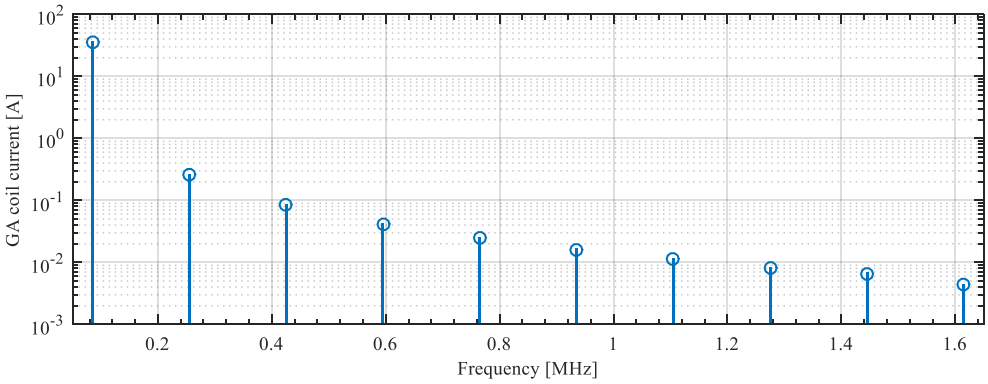

(**b**)

Figure 6. Transient current in the GA coil (**a**). Harmonics of the current in the GA coil (**b**).

3.3. Model Validation

The proposed procedure must be validated by answering the following two main questions: (1) Is the coupling with a DWPT coil system in the presence of an EV body modeled correctly? (2) Is MTL theory implemented correctly?

The validation of the proposed coupling model (question 1) was carried out considering a simplified configuration of the cable, which was here assumed to be a single conductor with the same diameter as the outer diameter of the MTL cable shield. The single conductor line had a length of l = 31.5 m. The excitation was produced by the DWPT coil system described above considering an EV placed above the GA coil at the mid of the line and absorbing 10 kW. This configuration was analyzed by a 3D FEM simulation and compared with the proposed MTL solution implemented in a MATLAB code.

The results in terms of current at the right end of the cable shield (armor) obtained by 3D FEM (single conductor) and MATLAB (MTL) simulations are shown in Figure 7a, showing a very good agreement and thus validating the coupling model.

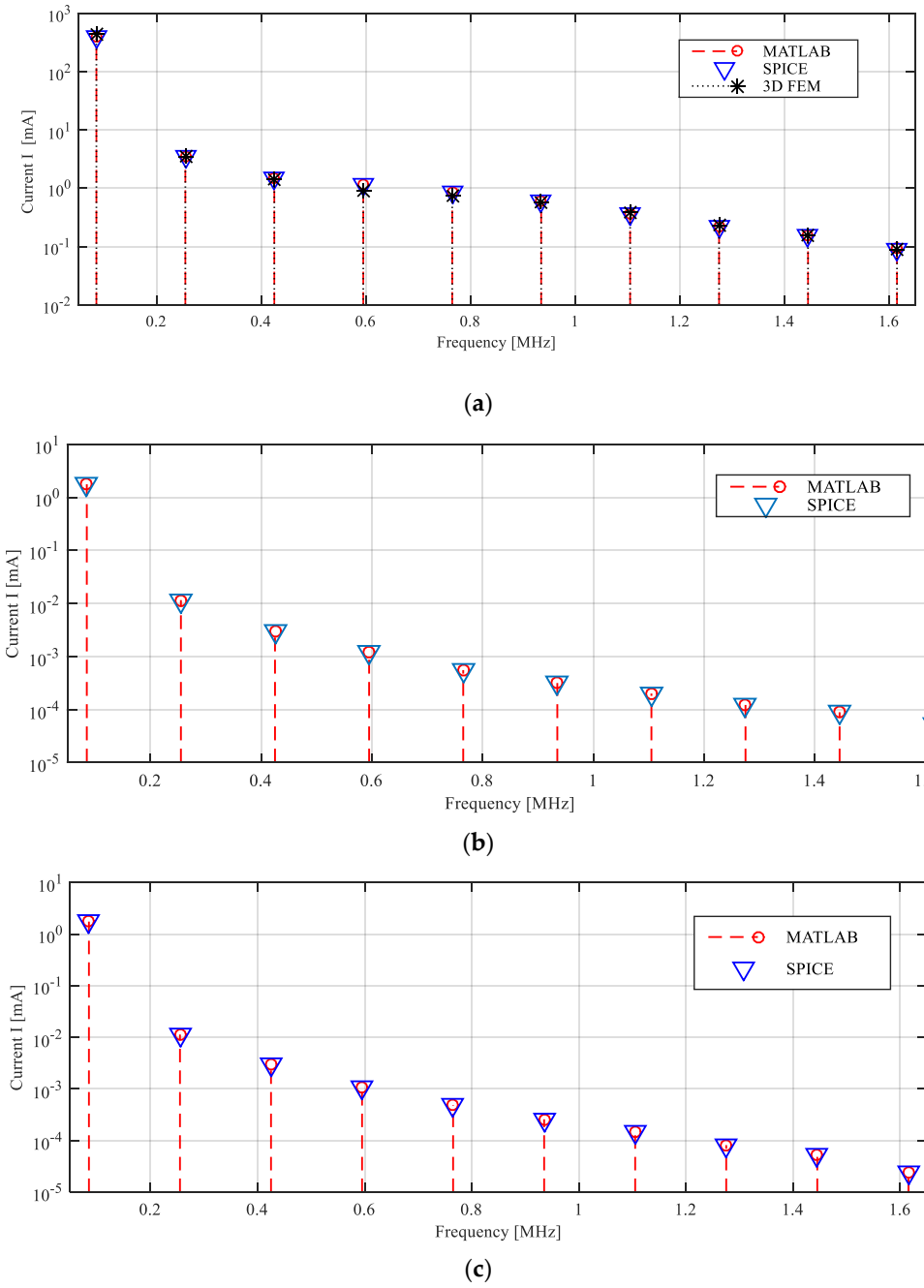

Figure 7. Comparison between the proposed MATLAB model and other models. Terminal current on left end: (**a**) armor (shield) current; (**b**) currents in internal lateral conductors no. 1–7 (see Figure 4), (**c**) current in internal central conductor no. 8.

To validate the MTL propagation model (question 2) we have compared the proposed MTL solution in MATLAB with that obtained by a SPICE simulation of a cable discretized in many MTL sections of 1.5 m length with lumped circuit elements [5]. The shield was terminated on a very small resistance (R_{term} = 100 pΩ) at both ends to simulate short-circuit conditions while all the internal conductors were all terminated on a resistance of 50 Ω at both ends. The results obtained are shown in Figure 7a–c showing a very good agreement.

We can observe that there is an extremely good agreement between the proposed MATLAB model, the SPICE model solution and the 3D FEM simulation for the terminal currents at the right end of the cable. The good agreement between the SPICE MTL model and the MATLAB model suggests that the solution is correctly implemented in MATLAB

while the good agreement between these solutions and the 3D FEM solution suggests that the source is adequately modeled in the proposed MTL model.

3.4. EMI Results

After its validation, the proposed procedure is applied to predict the induced effects in the traffic light cable described above. First, a cable of length l = 100 m is considered when a single EV is wireless charging by absorbing 10 kW on the electrified road at a distance x = 25 m (i.e., $\frac{1}{4}$ of the length) from the left side of the cable. The current in the external shield of the cable has a value of 47.3 mA on the left end and 264.5 mA on the right end at 85 kHz. For the higher order harmonics, the current declines.

Using the proposed method, the currents in the internal conductors of the MTL cable are calculated. As terminal conditions on the left and right side, 50 Ω resistances are used for each internal conductor. The currents in the internal conductors of the MTL cable are shown in Figure 8. It can be noted that the currents in conductors no. 1–7 are identical while the current in the central conductor (no. 8) is smaller. At the frequency of 85 kHz, the terminal current has a value of just under 1.6 mA, while it is significantly lower for higher order harmonics. The inner conductor-shield voltages at the left termination are shown in Figure 9.

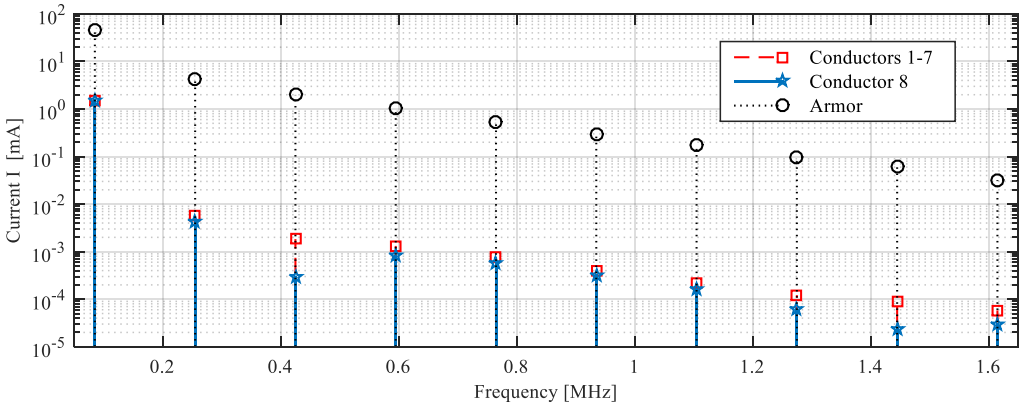

(**a**)

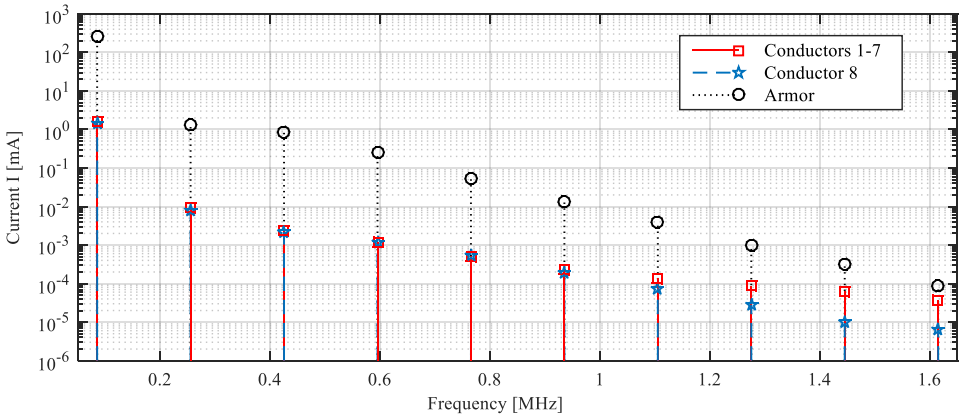

(**b**)

Figure 8. Terminal currents in the shield (armor) and in the inner wires of the buried MTL cable with one charging EV located at x = 25 m: (**a**) left end currents; (**b**) right end currents.

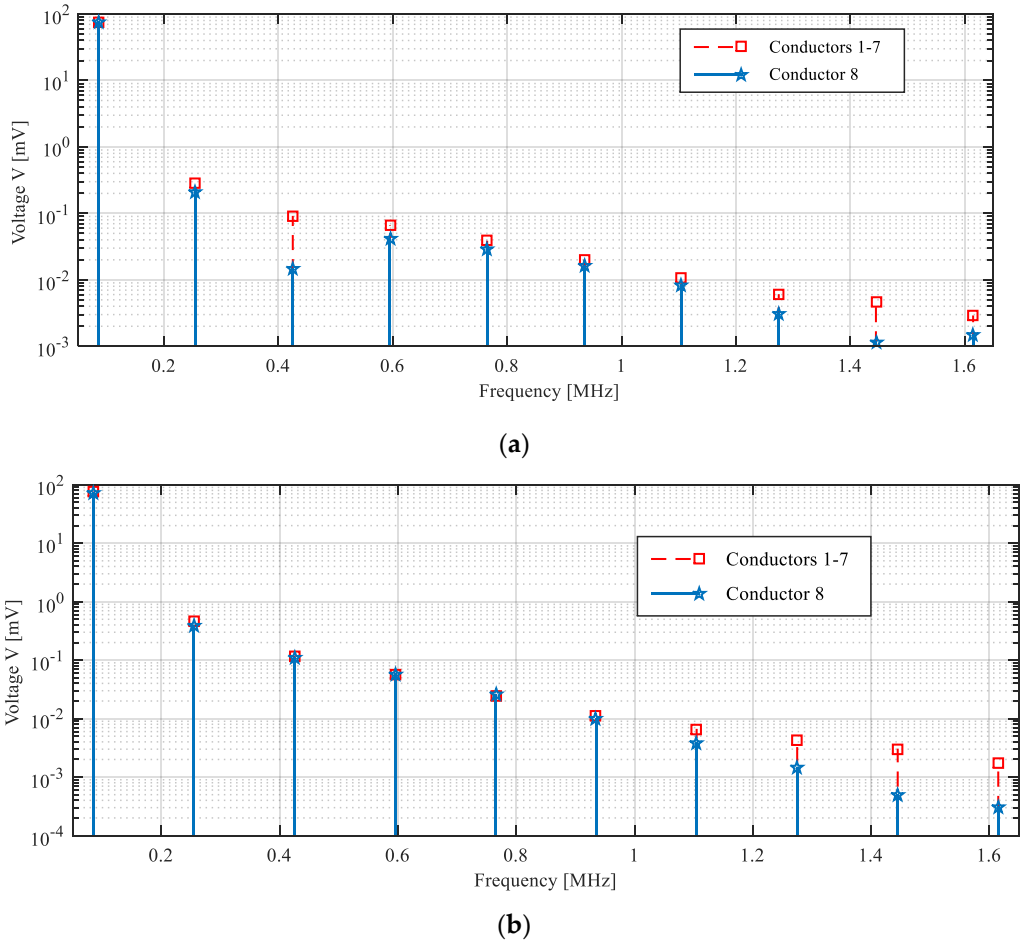

Figure 9. Terminal inner wire-to-shield voltages of the buried MTL cable with one charging EV located at x = 25 m calculated with the proposed method: (**a**) left end voltages; (**b**) right end voltages.

The proposed model can be easily modified to consider more EVs being charged. A cable length l = 100 m is considered with 10 equally spaced EVs along the electrified road. The transmitting GA coils are located at positions along the x-axis: $x_K = K(l + l_{GA})/(N_{car} + 1) - l_{GA}/2$, x_K being the centers of the Kth transmitting coil and $y = z = 0$ for K = 1,2, . . . , N_{car}, being N_{car} = 10 in the considered case. A power of 10 kW is transferred to each of the 10 EVs considered for a total of 100 kW.

The terminal currents on the left and right ends of the shield and in the inner wires are shown in Figure 10. We can observe that the level of the current decreases with the order of harmonic, as expected. The terminal inner wire-to-shield voltages, considering the internal conductors each loaded on a resistance of 50 Ω and the shield terminated on a resistance close to zero (short circuit), are shown in Figure 11. From these results, it can be noted that the values of currents and voltages on the terminations are the same since the source are symmetrically placed with respect to the terminations. The highest current is obtained at the first frequency, 85 kHz, with a value of 1.25 A in the armor, 16.1 mA in the inner central conductor no.8 while the inner lateral conductors no. 1–7 have a current of 16.7 mA. For the internal conductors at the higher frequencies we have values lower than 76 μA for 255 kHz and lower values for higher frequencies. The terminal inner wire-to-shield voltages on the internal conductors have values of 0.8 V at 85 kHz while at 255 kHz it is below 3.8 mV. The calculated voltage levels are not very low and require further investigation. In conclusion, we can say that the application of a DWPT system involves possible EMI problems in the underground cables near the electrified road.

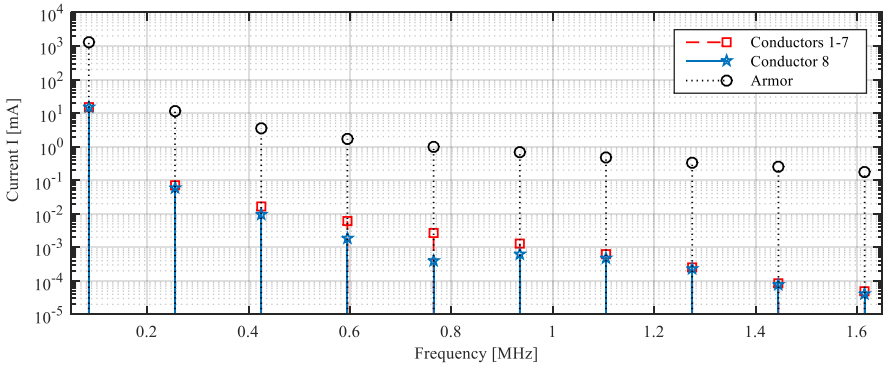

(**a**)

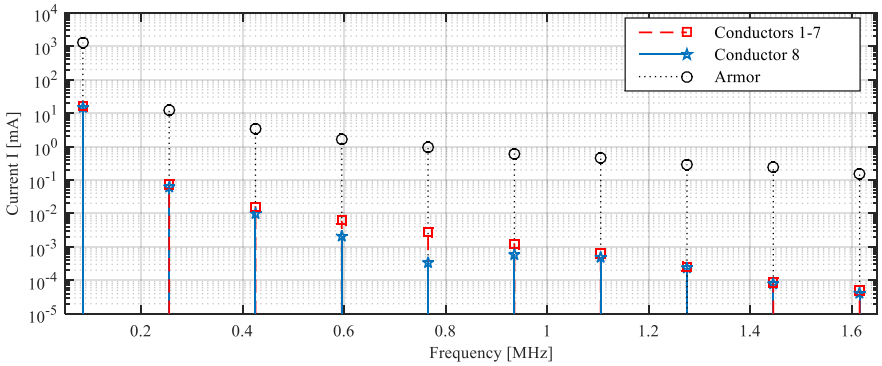

(**b**)

Figure 10. Terminal currents induced on the inner wires of a buried multiconductor cable for 10 charging EVs: (**a**) left end currents; (**b**) right end currents.

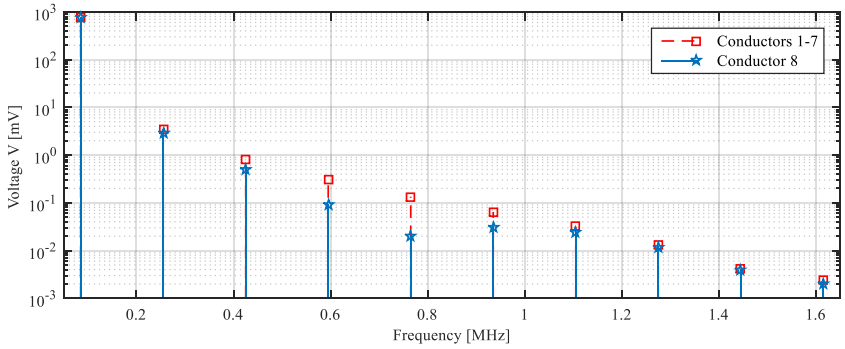

(**a**)

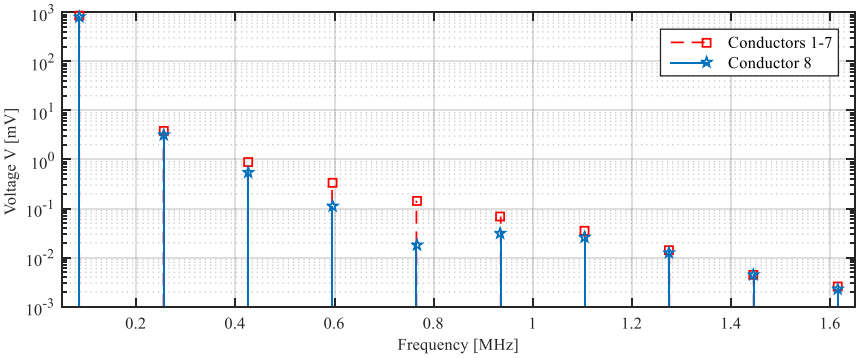

(**b**)

Figure 11. Terminal inner wire-to-shield voltages induced on a buried MTL cable for 10 charging EVs: (**a**) left end voltages; (**b**) right end voltages.

4. Conclusions

In this study, a method for predicting the induced currents and voltages produced by a DWPT system for an automotive on an underground MTL cable was presented. The theory of an excited MTL in the field has been adopted. The effects induced on an MTL signal cable were calculated up to 10 higher order harmonics of the fundamental frequency of 85 kHz. For the purpose of validation, the results of the proposed model of the underground MTL cable were compared with the results obtained with other methods, revealing a very satisfactory agreement.

The main scientific novelty of this study lies in the MTL model of the coupling between DWPT coils and underground cables. The results obtained are also completely new because the DWPT systems are not yet implemented, but only experimental tests have been carried out with the main purpose of wireless charging electric vehicles in motion, while EMC studies as proposed here have not yet been performed.

The limitations of the proposed MTL model are the well-known ones of the transmission line theory, given mainly by negligible radiation. However, this limitation is clearly satisfied for the examined buried cable-DWPT coil system configuration. Another limitation is given by the simplification of the coupling model between a DWPT coil with the buried cable. A small inaccuracy can also be given by the simplification of the coupling model between a DWPT coil with the buried cable. Obviously, in a real application in a high-density urban scenario, the hypothesis of a homogeneous earth is not entirely realistic and the presence of many conductive objects could alter the results obtained. However, the calculations made are very important to predict the possible collateral effects of a DWPT system deployment. Finally, the results obtained in this preliminary numerical investigation are not so satisfactory as to exclude possible EMI problems in buried cables due to DWPT systems.

Author Contributions: S.C., T.C., F.M. and M.F. conceived and planned the experiments and carried out the simulations. All authors provided critical feedback, improved the final design, analyzed the data and wrote the paper. All authors have read and agreed to the published version of the manuscript.

Funding: This research received no external funding.

Conflicts of Interest: The authors declare no conflict of interest.

References

1. Fabric European Project. Available online: https://cordis.europa.eu/project/id/605405 (accessed on 18 February 2022).
2. Buja, G.; Rim, C.; Mi, C.C. Dynamic Charging of Electric Vehicles by Wireless Power Transfer. *IEEE Trans. Ind. Electron.* **2016**, *63*, 6530–6532. [CrossRef]
3. Laporte, S.; Coquery, G.; Deniau, V.; De Bernardinis, A.; Hautière, N. Dynamic Wireless Power Transfer Charging Infrastructure for Future EVs: From Experimental Track to Real Circulated Roads Demonstrations. *World Electr. Veh. J.* **2019**, *10*, 84. [CrossRef]
4. Cruciani, S.; Campi, T.; Maradei, F.; Feliziani, M. Active Shielding Applied to an Electrified Road in a Dynamic Wireless Power Transfer (WPT) System. *Energies* **2020**, *13*, 2522. [CrossRef]
5. Paul, C.R. *Analysis of Multiconductor Transmission Lines*; Wiley-IEEE Press: Hoboken, NJ, USA, 2007.
6. Cristina, S.; Feliziani, M. A finite element technique for multiconductor cable parameters calculation. *IEEE Trans. Magn.* **1989**, *25*, 2986–2988. [CrossRef]
7. Ametani, A. A general formulation of impedance and admittance of cables. *IEEE Trans. Power Appar.* **1980**, *99*, 902–920. [CrossRef]
8. Jackson, J.D. *Classical Electrodynamics*; John Wiley & Sons, Inc.: New York, NY, USA, 1999.
9. Jin, J.-M. *The Finite Element Method in Electromagnetics*; John Wiley & Sons, Inc.: New York, NY, USA, 2002.
10. Cruciani, S.; Maradei, F.; Campi, T.; Feliziani, M. Dynamic Wireless Power Transfer in Urban Area: EMI on Traffic Signal Cables. In *2021 Asia-Pacific International Symposium on Electromagnetic Compatibility (APEMC)*; IEEE: Piscataway, NJ, USA, 2021; pp. 1–4. [CrossRef]
11. Caniggia, S.; Maradei, F. SPICE-Like Models for the Analysis of the Conducted and Radiated Immunity of Shielded Cables. *IEEE Trans Electromagn. Compat.* **2004**, *46*, 606–616. [CrossRef]
12. Feliziani, M.; Maradei, F. Full wave analysis of shielded cable configurations by the FDTD method. *IEEE Trans. Magn.* **2002**, *38*, 761–764. [CrossRef]

13. Taylor, C.D.; Sattenvhite, R.S.; Harrison, C.W. The response of a terminated two wire transmission line excited by a nonuniform electromagnetic field. *IEEE Trans. Antennas Propagat.* **1965**, *13*, 987–989. [CrossRef]
14. Theethayi, N.; Thottappillil, R.; Paolone, M.; Nucci, C.; Rachidi, F. External impedance and admittance of buried horizontal wires for transient studies using transmission line analysis. *IEEE Trans. Dielectr. Electr. Insul.* **2007**, *14*, 751–761. [CrossRef]
15. Wedepohl, L.M.; Wilcox, D.J. Transient analysis of underground power-transmission systems. System-model and wave-propagation characteristics. In Proceedings of the Institution of Electrical Engineers; IET Digital Library: London, UK, 1973; Volume 120, pp. 253–260. [CrossRef]
16. Vance, E.F. *Coupling to Shielded Cables*; John Wiley and Sons: New York, NY, USA, 1978.
17. Saad, O.; Gaba, G.; Giroux, M. A closed-form approximation for ground return impedance of underground cables. *IEEE Trans. Power Deliv.* **1996**, *11*, 1536–1545. [CrossRef]
18. Ametani, A.; Yoneda, T.; Baba, Y.; Nagaoka, N. An Investigation of Earth-Return Impedance Between Overhead and Underground Conductors and Its Approximation. *IEEE Trans Electromagn. Compat.* **2009**, *51*, 860–867. [CrossRef]
19. Poljak, D.; Doric, V.; Rachidi, F.; Drissi, K.E.K.; Kerroum, K.; Tkachenko, S.V.; Sesnic, S. Generalized Form of Telegrapher's Equations for the Electromagnetic Field Coupling to Buried Wires of Finite Length. *IEEE Trans Electromagn. Compat.* **2009**, *51*, 331–337. [CrossRef]
20. Campi, T.; Cruciani, S.; Maradei, F.; Feliziani, M. Magnetic Field Generated by a 22 kW-85 kHz Wireless Power Transfer System for an EV. In Proceedings of the 2017 AEIT International Annual Conference (AEIT), Cagliari, Italy, 20–22 September 2017; pp. 1–4.
21. Campi, T.; Cruciani, S.; De Santis, V.; Maradei, F.; Feliziani, M. EMC and EMF safety issues in wireless charging system for an electric vehicle (EV). In Proceedings of the 2017 International Conference of Electrical and Electronic Technologies for Automotive, Turin, Italy, 15–16 June 2017. [CrossRef]
22. Campi, T.; Cruciani, S.; De Santis, V.; Maradei, F.; Feliziani, M. Numerical Characterization of the Magnetic Field in Electric Vehicles Equipped with a WPT System. *Wirel. Power Transf.* **2017**, *4*, 78–87. [CrossRef]
23. COMSOL Multiphysics. Available online: https://www.comsol.com (accessed on 18 February 2022).
24. Feliziani, M.; Maradei, F. Edge element analysis of complex configurations in presence of thin shields. *IEEE Trans. Magn.* **1997**, *33*, 1548–1551. [CrossRef]
25. Feliziani, M.; Maradei, F. Fast computation of quasi-static magnetic fields around nonperfectly conductive shields. *IEEE Trans. Magn.* **1998**, *34*, 2795–2798. [CrossRef]